Z. Phys. Chem. **224** (2010) 263–278 / **DOI** 10.1524/zpch.2010.6104
© by Oldenbourg Wissenschaftsverlag, München

Hydrogen Dynamics in Lightweight Tetrahydroborates

By Arndt Remhof[1,*], Robin Gremaud[1], Florian Buchter[1], Zbigniew Łodziana[1], Jan Peter Embs[2], Timmy A. J. Ramirez-Cuesta[3], Andreas Borgschulte[1], and Andreas Züttel[1]

[1] Empa, Swiss Federal Institute for Materials Testing and Research, Überlandstrasse 129, CH-8600 Dübendorf, Switzerland
[2] Laboratory for Neutron Scattering ETH Zürich & Paul Scherrer Institut, WHGA 112, CH-5232 Villigen - PSI, Switzerland
[3] ISIS Facility, Rutherford Appleton Laboratory, Building R3, Room 1–42, OX11 0QX Chilton, Didcot, Oxon, United Kingdom

(Received March 30, 2009; accepted August 17, 2009)

Hydrogen / Dynamics / Tetrahydroborates

The high hydrogen content in complex hydrides such as $M[AlH_4]_x$ and $M[BH_4]_x$ (M = Li, Na, K, Mg, Ca) stimulated many research activities to utilize them as hydrogen storage materials. An understanding of the dynamical properties on the molecular level is important to understand and to improve the sorption kinetics. Hydrogen dynamics in complex hydrides comprise long range translational diffusion as well as localized motions like vibrations, librations or rotations. All the different motions are characterized by their specific length- and timescales. Within this review we give an introduction to the physical properties of lightweight complex hydrides and illustrate the huge variety of dynamical phenomena on selected examples.

1. Introduction

The understanding of the hydrogen dynamics is one of the most exciting challenges in the research on metal-hydrogen systems; its knowledge is a starting point to describe phenomena like optical, electronic and transport properties and mechanisms, and thermodynamics. In (d-metal) hydrides, these phenomena can be satisfyingly approximated within one-electron pictures [1] assuming hydrogen on interstitial sites in the metallic host lattice. Accordingly, the electronic structure changes are similar to those caused by alloying of two metals [2], and the

* Corresponding author. E-mail: arndt.remhof@empa.ch

vibrational properties of e.g. $PdD_{0.63}$ are text book examples of phonon dispersions of lattice vibrations in a binary compound [3].

Recently, complex metal hydrides containing BH_4^- ions have gained attention as hydrogen storage materials [4]. Thereby the hydrogen bond has a completely different chemical character than in the metal hydrides. Thus the above mentioned classical models on hydrogen in metals are not valid anymore.

Compounds containing the tetrahydroborate ion BH_4^- are extensively used reagents, both in inorganic and organic synthesis as well as in organo-metallic chemistry [5–7]. Alkali and alkaline earth tetrahydroborates form colorless solids, typically supplied as white powders or pellets. They may be solved in organic solvents such as tetrahydrofuran (THF). Research on lightweight tetrahydroborates started in world war II during the attempt to find new volatile uranium compounds [8]. Due to their large volumetric and gravimetric hydrogen density they were proposed as solid rocket fuel [9] or as promising candidates for hydrogen storage [10]. However, their utilization is hindered by slow sorption kinetics and/or by a high thermodynamic stability, leading to high hydrogen desorption temperatures. Thermal desorption of the tetrahydroborates generally follow

$$M(BH_4)_x \rightarrow MH_x + B + \frac{3x}{2}H_2 \tag{1}$$

Diborane (B_2H_6) [11] and generally compounds containing B_xH_y have been found as unwanted decomposition by-products [12–16].

While the dynamics of H in many metallic systems is well understood, only rudimentary knowledge exists for the dynamics of hydrogen in complex hydrides. The reason for this originates from the different structures of the hydrides. Hydrogen in most transition metals occupies interstitial sites and hydrogen can easily jump from interstitial to interstitial, especially in understoichiometric compounds. Accordingly, the diffusion of hydrogen in transition metals is fast with small activation energies. Hydrogen in complex hydrides, on the contrary, is covalently bound to the other element like Al or B, and arranged in subunits ('complexes'). The hydrogen dynamics in such a system comprises the internal H - vibrations, within each complex, the rotation of the complex about specified axes, the motion of the BH_4 units against the metal ions (external H-vibrations) and the diffusion of hydrogen. In order to understand and to improve the hydrogen sorption kinetics, a detailed knowledge of the dynamical properties and the diffusion mechanisms within these lightweight hydrogen storage materials is crucial.

This review is intended to give an introduction to the tetrahydroborates and to illustrate their rich dynamical properties on some recent experimental results having important consequences on the understanding of the physics and chemistry of hydrogen storage in complex hydrides. Starting from the structural properties we discuss the rotational and vibrational motion of the complex anion as well as the sorption mechanism and hydrogen transport.

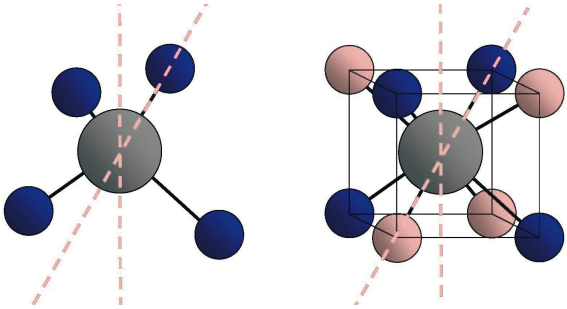

Fig. 1. BH_4 tetrahedron (left panel), spatial arrangement of the two possible hydrogen tetrahedra (right panel, light and dark) around the central B atom. The positions of the high symmetry axes are indicated as dashed lines.

2. Structural properties

At ambient conditions the tetrahydroboranates of the monovalent alkali metals, except $LiBH_4$, crystallize in a cubic NaCl- like structure, consisting of positively charged metal cations and negatively charged $[BH_4]^-$ anions. Within the BH_4 subunits the hydrogen is located at the corners of a tetrahedron, surrounding the boron. As displayed in figure 1, the hydrogen atoms thereby occupy four out of eight corners of a cube around the B atom, leaving the next nearest corners unoccupied. This implies a random distribution of BH_4^- tetrahedra in two different < 111 > orientations along cube diagonal in the high temperature, disordered phase. There are two sets of high symmetry axes connected with this structure, which are indicated by dashed lines in figure 1. First, there are three 2-fold axes, called c2, which are normal to the cube's face and four 3-fold axes, called c3, which coincide with the body diagonals of the cube. The two possible arrangements may be transferred in one another by a 90° rotation around c2 axis, while a rotation about c3 axis preserves the tetrahedron's orientation, as depicted in Fig. 1.

The reorientational transition between the two different orientations will be discussed in the next section. $LiBH_4$ at room temperature crystallizes in the orthorhombic Pnma structure (space group no. 62). Heat capacity studies for the MBH_4 series with M = Na, K, Rb, Cs suggest phase transitions at 190K for $NaBH_4$, 76K for KBH_4, 44K for $RbBH_4$ and 27K for $CsBH_4$, respectively [17]. The low temperature phases of $NaBH_4$ and KBH_4 have been determined to be ordered tetragonal structures, where one of the BH_4 orientation is "frozen" [18,19]. In the case of $RbBH_4$ and $CsBH_4$ no diffraction evidence for a lowering of structural symmetry has been found [19]. $LiBH_4$ undergoes a structural phase transition to a hexagonal high-temperature (HT) structure around 380 K [20]. Diffraction studies have pointed out a dramatic increase in hydrogen or deuterium thermal displacements by almost 2 orders of magnitude from 4 to 400 K [21,22], which was attributed to dynamical disorder in the HT phase [23].

The increased disorder also strongly influences the phonon spectrum of the crystal. The phonon density of states (PDOS) of the LT phase depends quadratically on the phonon energy as expected by the Debye theory for acoustic vibrations in crystalline solids, while the HT phase shows a linear dependence of the PDOS as a function of the phonon energy [22].

The excess of density of states of the high-T phase reveals a high lattice anharmonicity and it is a characteristic feature of glasses and disordered systems [22]. The dynamics of $LiBH_4$ have also been studied by nuclear magnetic resonance spectroscopy (NMR). Recent studies by Matsuo et al. [41] and Corey et al. [42] reveal a sudden line-narrowing of the ^{7}Li resonance at the phase transition point, indicative of a a rapid lithium diffusion in the high-T phase. Thereby hopping rates of 10^9 jumps/s have been observed. The NMR-determined hopping is in agreement with large ionic electrical conductivity [41].

Apart from the ambient pressure phases, several high pressure phases have recently been revealed for $LiBH_4$ [28] and $NaBH_4$ [26]. All phase transitions in the monovalent tertrahydroborates were reported to be fully reversible.

While there are extensive studies on the alkali tetrahydroborates, much less is known about the structure and the dynamics of the divalent alkaline earth tetrahydroborates. They crystallize in more complex crystal structures with unit cells for $Mg(BH_4)_2$ comprising up to 330 atoms in $P6_1$ symmetry[31, 32, 43–46]. Depending on the sample preparation and treatment several phases have been found to coexist at room temperature. For $Ca(BH_4)_2$ three phases are well established by diffraction experiments and calculations [34,35,39]. Even though several phase transitions between those phases have been observed in the past, the complete phase diagrams are still to be discovered. Table 1 lists the known structures together with the structures of their monovalent relatives. Analogous to the behavior observed for the alkali tetrahydroborates, reorientational motions of the $[BH_4]^-$ ion have been observed [47].

3. Rotational motion of BH_4^- in $NaBH_4$

In a combined experimental and theoretical study the rotational motion of the BH_4 tetrahedra in $NaBH_4$ by means of incoherent quasielasic neutron scattering (QENS) and density functional theory (DTF) calculations were investigated [48].

QENS measurements were carried out using the time-of-flight neutron spectrometer FOCUS for cold neutrons located at the continuous spallation source SINQ at the Paul Scherrer Institute in Villigen, Switzerland [49,50].

Generally, the scattering function can be written as [51]

$$S(Q,\omega) = A_0(Q)\delta(\omega) + \sum A_j(Q)L_j(\omega) \tag{2}$$

where $A_0(Q)$ is the elastic incoherent structure factor *EISF*, $\delta(\omega)$ represents the elastic term with zero energy width, and L_j are the quasielastic contributions each with its own quasielastic incoherent structure factor $A_j(Q)$. If the resolution

Table 1.

	Space Group	a	b (β)	c	T	Ref
		(Å)	(Å)(°)	(Å)	(K)	
$LiBH_4$	*Pnma*	7.17858(4)	4.43686(2)	6.80321(4)	293	[20]
		7.1730(1)	4.4340(1)	6.7976(1)	298	[24]
		7.1213(2)	4.4060(1)	6.6744(2)	3.5	[21]
		7.141(5)	4.431(3)	6.748(4)	225	[25]
		7.1160(5)	4.4056(4)	6.6730(5)	10	[22]
	$P6_3mc$	4.27631(5)		6.94844(8)	408	[20]
		4.2667(2)		6.9223(8)	400	[21]
		4.3228(10)		7.0368(10)	535	[25]
	*Ama*2	6.4494(9)	5.307(1)	5.2919(9)	293*	[26]
	Fm[3]*m*	5.109(2)			293f	[26]
$NaBH_4$	*Fm*[3]*m*	6.148(1)			293	[18]
		6.1308(1)			200	[27]
	$P[4]2_1c$	4.332(1)		5.869(1)	10	[18]
	Pnma	7.297(1)	4.1166(5)	5.5692(7)	293 f	[28]
KBH_4	*Fm*[3]*m*	6.728(1)			293	[29]
		6.7306(1)			295	[19]
	$P4_2/nmc$	4.7004(2)		6.5979(3)	10	[19]
$Be(BH_4)_2$	$I4_1cd$	13.62(1)		9.10(1)	293	[30]
$Mg(BH_4)_2$	$P6_1$	10.3182(1)		36.9983(5)	293	[31]
		10.3414 (4)		37.086 (2)	293	[32]
	$P6_122$	10.3540(12)		37.055(4)	100	[33]
	Fddd	37.072(1)	18.6476(6)	10.9123(3)	293	[32]
$Ca(BH_4)_2$	*Fddd*	8.791(1)	13.137(1)	7.500(1)	293	[34]
		8.7461(8)	13.0942(9)	7.4660(7)	300	[35]
	*F*2*dd*	8.7759(3)	13.0234(4)	7.4132(2)	91	[36]
	$P4_2/m$	6.9468(1)		4.3661(4)	480	[35]
		6.9241(2)		4.3492(1)	293	[37]
	P[4]	6.91894(11)		4.34711(12)	305	[36,38]
	I[4]2*d*	5.8446(3)		13.2279(11)	495	[36]
	Pbca	13.0584(8)	8.3881(4)	7.5107(4)	300	[39]
$Al(BH_4)_3$	$C2/c$	21.917(4)	5.986(1)	21.787(4)	150	[40]
			β = 111.90(3)			
	$Pna2_1$	18.021(3)	6.138(2)	6.1987(14)	195	[40]

* 2.4 GPa
f 18.1 GPa
f 11.2 GPa

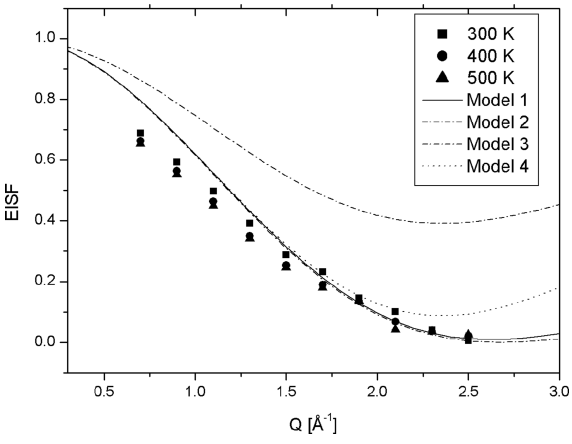

Fig. 2. Measured EISFs (solid symbols) for $NaBH_4$, compared to different model calculations: 90° reorientations (model 1), free rotator (model 2), two side and three side jump model (model 3) and reorientation of the C3 axis (model 4).

broadened elastic line and the quasielastic component can be experimentally separated, the EISF is a measurable quantity which can be expressed as

$$EISF(Q) = \frac{I_{el}(Q)}{I_{el}(Q) + I_{qe}(Q)} \tag{3}$$

where $I_{el}(Q)$ and $I_{qe}(Q)$ are the integrated elastic and quasielastic intensities. Figure 2 displays the measured EISF with several models described below. The case of the orientationally disordered $NaBH_4$ may be treated in analogy to the ammonium halides such as NH_4Cl, NH_4Br or NH_4I, which are classical examples of solid rotor phases. Lechner et al. [52] describe the rotational motion of the NH_4 ion in NH_4Br by a model corresponding to 90° reorientations (model 1). In this case, the EISF can be expressed as

$$EISF(Q) = \frac{1}{8}[1 + 3j_0(Qa) + 3j_0(QA\sqrt{2}) + j_0(QA\sqrt{3})] \tag{4}$$

where $j_0(x) = \sin(x)/x$ is the 0th order Bessel function. The same model also reproduces the EISF measured at $NaBH_4$. The only fit parameter thereby is the H-H distance a. The fit yields a = 1.35 Å, corresponding to a B-H distance of r = 1.17 Å which coincides nicely with the B-H distance measured by neutron diffraction [18].

Within the accessible Q-range and the resolution of the instrument, model 1 is indistinguishable from the free rotation (model 2). Other possible models are the two-site jump model (model 3), in which the BH_4 ion rotates around one of the c2 axes, the three-site jump model around one of the c3 axes (which results also in model 3) or the tetrahedral jump model, which describes reorientations of the c3 axis (model 4), can be excluded. A detailed description of the models

is given by by Jalarvo et al. [53]. We attribute the deviation at low Q to multiple scattering, which enhances the inelastic part for small angles.

The observed broadening was found to be independent of Q and displays a thermally activated Arrhenius behavior. The measured value of the activation energy of E_a = 117(1) meV, corresponding to 10.9(0.1) kJ/mol fits nicely to the value of 11.2(0.5) kJ/mol obtained by NMR spectroscopy [54] and the value of 12.1(0.5)kJ/mol measured by Raman spectroscopy [23].

The reason why 90° reorientational motions are preferred to other possible rotations lies in the height of the energy barrier that has to be overcome. Based on a plane wave formulation of density functional theory (DFT) [55], where atomic cores were represented by projected augmented waves potentials [56], the potential energy for rotation of a single BH_4 tetrahedron within the HT structure of $NaBH_4$ was calculated. The calculations were performed in the supercell geometry with 96 atoms to minimize errors due to periodic boundary conditions. To model adiabatic rotation no atomic relaxation was performed during rotation of single BH_4 unit. In the course of potential energy landscape calculations all BH_4 tetrahedra, except the rotated one, were fixed. In this initial configuration the nearest BH_4 neighbors within the (a,b) plane are oriented in the antiparallel fashion (rotated by 90°), while they are aligned along the c-axis. Figure 3 shows the calculated two dimensional representation of the potential energy surfaces for rotational motions around the c2 (parallel to the crystallographic c-axis) and subsequent rotation around c3 axes (Fig. 3(top panel)). Fig. 3(bottom panel) depicts the energy landscape for the c2 rotation followed by another c2 rotation around a perpendicular axis. The origin of the coordinate system was chosen such that (0,0) corresponds to the energy of the initial state. As expected from the symmetry, further minima occur at c2 = 90°, c2 = 180° and at c2 = 270° as well as at c3 = 120° and at c3 = 240° for c2/c3 axis rotation respectively. For rotation around c2 axes eight minima can be distinguished. Thereby the local minima at c2 = 90° and at c2 = 270°, are representing the parallel alignment of the rotated BH_4 tetrahedron with respect to the initial state (i.e. the same BH_4 orientation as for all nearest neighbors in (a,b) plane). These minima are less pronounced than the minima at c2 = 0° and at c2 = 180°, representing the initial lowest energy state case. The calculation yields a barrier height ~ 210 meV for the reorientation around c2 axis between two distinguished global energy minima, while the escape barrier from the local minima is ~ 110 meV.

In the real crystal, at finite temperature, there is an even distribution of BH_4 orientations, such that all orientations are equivalent. Energetically, both positions will be degenerated and from the energetic point of view, the $c2$-axis will have 4-fold $c4$ symmetry. The height of the barrier for reorientation will be in between the two extreme cases. Relaxation processes of the surrounding tetrahedra might slightly lower the barrier, however fast reorientation process will be close to adiabatic one, as in the present calculations. The barrier height for a rotation around a $c3$ axis is ~ 320 meV and it is larger than for $c2$ axis. Therefore, we would expect a preferred rotation around the $c2$ axes. This also can be under-

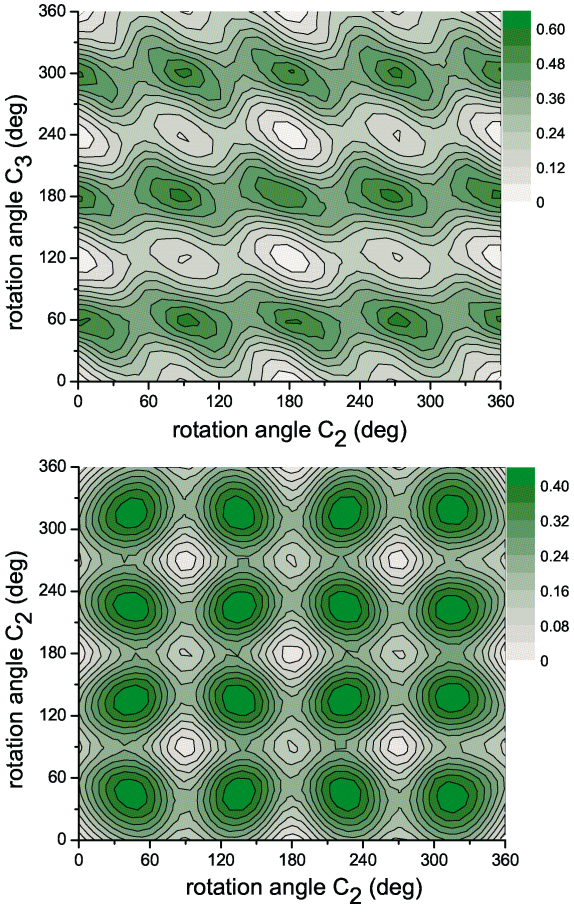

Fig. 3. Top panel: Calculated two dimensional representation of the potential energy surfaces for rotational motions of a BH_4 tetrahedron in $NaBH_4$ around the c2 (parallel to the crystallographic c-axis) and subsequent rotation around c3 axes. Bottom panel: Corresponding energy landscape for the rotation about two perpendicular c2 axes. The scale is in eV.

stood by the fact, that rotation around c2 axis do not change orientation of BH_4 with respect to metal cations, i.e. number of hydrogen atoms pointing toward Na remains remains equal to two, while the rotation around c3 axis include unfavorable monodentate orientation with one hydrogen pointing directly toward sodium.

4. BH_4^- vibrations

In the tetrahydroborates, the pseudo-molecule BH_4^- is ionically bound to the counter ion. Therefore phonons can be well approximated by so-called 'internal' and 'external' vibrations [23,57,58], where 'internal' refers to the characteristic vibrations of the BH_4^- ion, and 'external' refers to the vibrational properties of the whole crystal structure. Accordingly, the labeling $\nu_{1,...,4}$ of the internal vibrations is based on the vibrational modes of a free BH_4^- tetrahedral molecule, as the effect of the crystal field is small.

The three complementary techniques of vibrational spectroscopy, i.e. inelastic neutron scattering (INS) [59,60], Raman scattering [23,47,61,62] and infrared spectroscopy [19,58] are used to characterize BH_4^- in tetrahydroborates, but also in solution [27,63] or in a solid matrices [64]. Recently, the inelastic scattering of synchrotron X-ray radiation has been used to characterize the low-lying phonons in $NaBH_4$ [65].

As an example, we show here the vibrational spectra of $LiBH_4$ in fig. 4. The spectra can be schematically divided in 6 regions, numbered from I to VI as shown in fig. 4. Region I corresponds to the external vibrations. At the lowest energies are the translational lattice vibrations, where the whole BH_4^- moves against the Li^+ ion. Phonons originating from librational motions -also called constrained rotations- of the BH_4^- units appear at higher energies, e.g. as a large band from 38 to 59 meV in the INS spectrum. The same region (300–475 cm^{-1})is also weakly active in the Raman spectrum, and is attributed in this case to a combination band of the bending and librational vibrations [61]. Internal vibrations of the BH_4^- unit are found in region III (B-H bending) and V (B-H stretching). The narrow internal vibration peaks measured by INS reflect limited dispersion of the BH_4^- phonon density of state. Finally, the broad features observed in region II, IV and VI originate from overtones and combination bands. The comparatively high peak intensities at 2157 and 2173 cm^{-1} in the Raman spectrum arise from Fermi resonances between the stretching modes and the first overtones of the bending modes [62,66].

By recording the width of Raman modes upon temperature increase [61,67], the increase in dynamic disorder of the BH_4^- unit can be followed. As seen in fig. 5, an abrupt increase in disorder occurs at the transition from the low to the high temperature phase that can be modeled by DFT [22] in term of lower rotational reorientation barriers in the high temperature than in the low temperature phase.

5. Sorption mechanism of complex hydrides probed by vibrational spectroscopy

The consideration of complex hydrides as hydrogen storage materials is a recent attempt, despite the fact that the compounds are known since decades. The reason

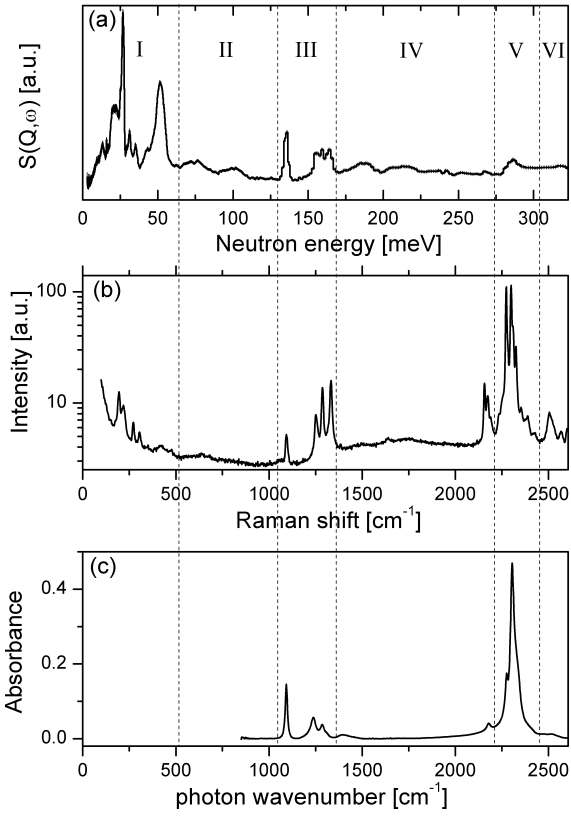

Fig. 4. (a) Inelastic neutron scattering (20 K), (b) Raman scattering (83 K) and (c) Fourier-transformed infrared spectroscopy (295 K) spectra of $LiBH_4$. Regions I to VI are discussed in the text.

for this is their extremely slow sorption kinetics. However, in 1996 Bogdanovic demonstrated a reversible sorption behavior of catalyzed sodium alanate being very similar to that of well known classical metal hydrides. Interestingly, the sorption reaction is only reversible under technically applicable conditions, if the material is doped with transition-metal compounds, most efficiently with titanium compounds[68–70]. A multitude of experimental and theoretical methods have been applied to unravel the mechanism of the formation and decomposition process of $NaAlH_4$ - so far without a conclusive model [71–81]. Furthermore, similar effective additives for other complex hydrides e.g. the borohydrides have not yet been found. The principally slow sorption mechanism of complex hydrides can be understood on the basis of the previous sections: complex hydrides decompose into several (at least two, see e.g. reaction) solid phases and the hydrogen is covalently bound in subunits (e.g. BH_4). That means that in addition

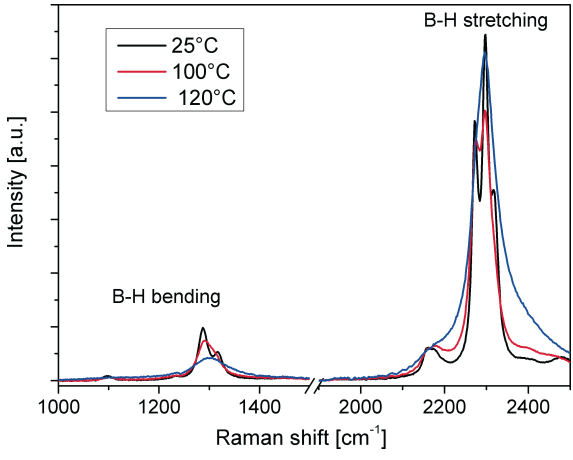

Fig. 5. $LiBH_4$ internal Raman modes for temperatures below (25°C, 100°C) and above (120°C) the structural phase transition.

to a slow hydrogen diffusion a mandatory but very slow metal atom diffusion hinders the formation and decomposition of complex hydrides. In this section, we want to highlight some of the results of the underlying research, in particular those which were gained from vibrational spectroscopy.

First step of the investigation of reaction mechanisms is the identification of all participating reactants. Due to the low crystallinity of the solid phases making identification difficult by diffraction methods, Raman spectroscopy was the first method indicating intermediate steps occurring during the decomposition of $LiBH_4$[13]. Furthermore, as vibrational spectroscopy is sensitive to vibrations irrespective wether they originate from lattice vibrations or molecular vibrations, vibrational spectroscopy are used to probe solid, liquid as well as gaseous states of complex hydrides. It is in line of thought of rigid molecular entities in $LiBH_4$ (see previous section) that the fingerprint of BH_4 units has been found in the gas phase of $LiBH_4$ (rotational spectrum measured by RF-absorption spectroscopy, Ref. [82]), in liquid $LiBH_4$ (stretching vibrations measured by Raman spectroscopy, Ref. [83]), in $LiBH_4$ dissolved in organic solvents (stretching vibrations measured by IR spectroscopy, Ref. [84]) and in solid $LiBH_4$ [62]. An important question related to the effect of additives is wether the additives interact with the hydrides. If they do, a change in the vibrational spectrum is expected. However, the Raman and infrared spectra of doped and undoped $NaAlH_4$ do not show striking differences, indicating a rather subtle effect of additives on $NaAlH_4$ [85]. On the other hand, Raman spectroscopy revealed the existence of yet unidentified species, which only occur during the decomposition of doped $NaAlH_4$ [79,86]. Thus, the additive seems to change the reaction path way. These experimental results are in good agreement with the model of Guynadin et al. explaining the

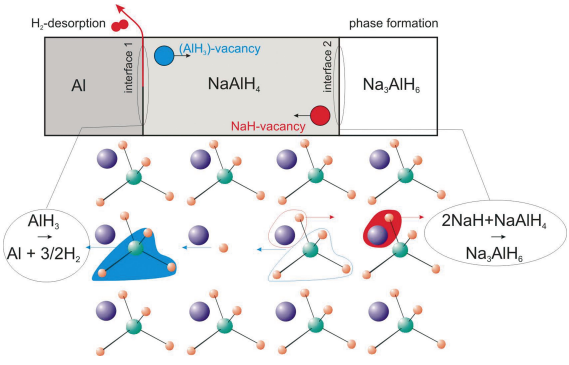

Fig. 6. Sketch of the decomposition reaction of $NaAlH_4$ via vacancy diffusion in $NaAlH_4$ (taken from Ref. [79]). Possible vacancies are e.g. charge neutral species like AlH_3 and NaH. At the interfaces, a vacancy is formed. This is filled up by the corresponding atoms from the inner, producing the same vacancy one layer deeper in the bulk. That way the vacancy moves through the crystal.

decomposition reaction via vacancy diffusion in $NaAlH_4$ [87]. The model of the decomposition reaction is illustrated in Fig. 6.

Hydrogen/deuterium exchange probed by vibrational spectroscopy is also used to probe the hydrogen transport mechanism in tetrahydroborates: recently we evidenced the presence of *all* partially exchanged $BH_{4-n}D_n$ units ($0 < n < 4$) in $LiBH_4$ exposed to deuterium gas below the melting temperature [83,88].

Although the motion of entire BH_4-units has been identified as the major mechanism for long range mass transport [42,89], the fact that D atoms are successively exchanged within the BH_4 units indicate that net transport of atomic hydrogen involves both, the transport of entire BH_4 units and the local H-exchange.

6. Outlook

The hydrogen in the p-element complex hydrides is covalently bound to boron or aluminum, forming a negatively charged ion. The hydrogen containing anion is ionically bond to the counter ion. Current research on these lightweight complex hydrides is stimulated by their potential use as hydrogen storage materials. In the last decade numerous experimental as well as theoretical studies have been carried out to understand and to improve the hydrogen transport and the sorption kinetics within these compounds. In these review the fundamental dynamical phenomena, comprising internal H - vibrations within each complex, reorientation of the complex about specified axes, the motion of the complex anion against the metal ions (external H-vibrations) and the diffusion of hydrogen, have been described.

Up to now, the dynamics of compounds were discussed as fingerprints to identify and characterize the complex hydrides themselves as well as the reactants during the hydrogen sorption cycle. The exciting question remains how the dynamics of complex hydrides is related to the reaction kinetics. The above discussed results treat the equilibrium or slightly perturbed states of matter (vibrations, diffusion). The explanation of reaction kinetics, though, must include the non-equilibrium states. The small displacement of atoms around their equilibrium positions might or might not be the precursor of e.g. a phase transformation. In $LiBH_4$, the softening of certain phonon modes has been interpreted as a precursor of the phase transformation at 110°C.[62] However, the measurement of the mandatory transition state is still an unsolved goal in solid state physics.[90] The development of new techniques and methods to measure the dynamics of the non-equilibrium state of matter is expected to reveal exciting new insights into the physics and chemistry of complex hydrides.

References

1. L. Schlapbach, F. Meli, and A. Züttel, in *Intermetallic Compounds, Principles & Practice*, (Eds.: J. H. Westbrook and R. L. Fleischer) John Wiley & Sons Ltd., Chichester (1994).
2. C. D. Gelatt, H. Ehrenreich, and J. A. Weiss, Phys. Rev. B **17** (1978) 1940; H. L. M. Bakker, R. Feenstra, R. Griessen, L. M. Huisman, and W. J. Venema Phys. Rev. B **26**, (1982) 5321; Smithson, H., C.A. Marianetti, D. Morgan, A. van der Ven, A. Predith, and G. Ceder, Phys. Rev. B **66** (2002) 144107.
3. J. M. Rowe, J. J. Rush, H. G. Smith, M. Mostoller, and H. E. Flotow, Phys. Rev. Lett. **33** (1974) 1297.
4. L. Schlapbach and A. Züttel, Nature (London) **414**, (2001) 353; G. W. Crabtree, M. Dresselhaus, and M. Buchanan, Physics Today **39** (2004); A. Züttel, A. Borgschulte, and L. Schlapbach *Hydrogen as a Future Energy Carrier*, Wiley-VCH, Weinheim, (2008).
5. L. F. Fieser and M. Fieser, *Reagents for Organic Synthesis*, Vol. 1–6, Wiley, New York (1962).
6. H. C. Brown, *Boranes in Organic Synthesis*, Cornell University Press, Ithaca, N. Y. (1972).
7. H. C. Brown, *Organic Synthesis via Boranes*, Wiley, New York (1975).
8. H. I. Schlesinger, H. C. Brown, B. Abraham, A. C. Bond, N. Davidson, A. E. Finholt, J. R. Gilbreath, H. Hoekstra, L. Horvitz, E. K. Hyde, J. J. Katz, J. Knight, R. A. Lad, D. L. Mayfield, L. Rapp, D. M. Ritter, A. M. Schwartz, I. Sheft, L. D. Tuck, and A. O. Walker, J. Am. Chem. Soc. **75** (1953) 186.
9. H. Kartluke, C. D. Mc Kinney, R. Pheasant, and W. B. Tarpley, Nasa, Final Report (1964).
10. A. Züttel, A. Borgschulte, and S. I. Orimo, Scripta Mater. **56**, (2007) 823.
11. S. Kato et al., to be submitted
12. O. Friedrichs, A. Borgschulte, S. Kato, F. Buchter, R. Gremaud, A. Remhof, and A. Züttel, Chemistry, Europ. J. **15** (2009) 5531.
13. N. Ohba, K. Miwa, M. Aoki, T. Noritake, S.-I. Towata, Y. Nakamori, S. I. Orimo, and A. Züttel, Phys. Rev. B **74** (2006) 075110.
14. J. Purewal, S.-J. Hwang, R. C. Bowman Jr., E. Rönnebro, B. Fultz, and C. Ahn, J. Phys. Chem. C **112** (2008) 8481.

15. S.-J. Hwang, R. C. Bowman Jr., J. W. Reiter, J. Rijssenbeek, G. L. Soloveichik, J.-C. Zhao, H. Kabbour, and C. C. Ahn, J. Phys. Chem. C **112** (2008) 3164.
16. V. Ozolins, E. H. Majzoub, and C. Wolverton, J. Am. Soc. Chem. **131** (2009) 230.
17. C. C. Stephenson, D. W. Rice, and W. H. Stockmayer, J. Chem. Phys. **23** (1955) 1960.
18. P. Fischer and A. Züttel, Mater. Sci. Forum **443–444**, (2004) 287.
19. G. Renaudin, S. Gomes, H. Hagemann, L. Keller, and K. Yvon, J. Alloy Compd. **375** (2004) 98.
20. J-Ph. Soulié, G. Renaudin, R. Cerný, and K. Yvon, J. Alloys Compd. **346** (2002) 200.
21. M. Hartman, J. Rush, T. Udovic, R. Bowman Jr., and S.-J. Hwang, J. Solid State Chem. **180** (2007) 1298.
22. F. Buchter, Z. Łodziana, Ph. Mauron, A. Remhof, O. Friedrichs, A. Borgschulte, A. Züttel, D. Sheptyakov, T. Strässle, and A. J. Ramirez-Cuesta, Phys. Rev. B **78** (2008) 094302.
23. H. Hagemann, S. Gomes, G. Renaudin, and K. Yvon, J.Alloys Comp. **363** (2004) 129.
24. A. Züttel, S. Rentsch, P. Fisher, P. Wenger, P. Sudan, Ph. Mauron, and Ch. Emmenegger, J. Alloys Compd. **356–357** (2003) 515.
25. Y. Filinchuk, D. Chernyshov, and R. Cerný, J. Phys. Chem. C. **112** (2008) 10579.
26. Y. Filinchuk, D. Chernyshov, A. Nevidomskyy, and V. Dmitriev, Angew. Chem. Int. Ed. **47** (2008) 529.
27. Y. Filinchuk and H. Hagemann, Eur. J. Inorg. Chem. **20** (2008) 3091.
28. Y. Filinchuk, A. Talyzin, D. Chernyshov and V. Dmitriev, Phys. Rev. B. **76** (2007) 092104.
29. R. L. Luck and E. J. Schelter, Acta Cryst. C. **55** (1999) IUC9900151.
30. D. S. Marynick and W. N. Lipscomb, Inorg. Chem. **11** (1972) 820.
31. R. Cerný, Y. Filinchuk, Y., H. Hagemann and K. Yvon, Angew. Chem. Int. Ed. **46** (2007) 5765.
32. J-H. Her, P. W. Stephens, Y. Gao, G. L. Soloveichik, J. Rijssenbeek, M. Andrus, and J.-C. Zhao Acta Crystallogr. Sect. B, **63** (2007) 561.
33. Y. Filinchuk, R. Cerný, and H. Hagemann, J. Phys. Chem. C. **21** (2009) 925.
34. K. Miwa, M. Aoki, T. Noritake, N. Ohba, Y. Nakamori, S. Towata, A. Züttel, and S. Orimo, Phys. Rev. B **74** (2006) 155122.
35. F. Buchter, Z. Łodziana, A. Remhof, O. Friedrichs, A. Borgschulte, Ph. Mauron, A. Züttel, D. Sheptyakov, G. Barkhordarian, R. Bormann, K. Chopek, M. Fichtner, M. Sørby, M. Riktor, B. Hauback, and S. Orimo, J. Phys. Chem. B **112** (2008) 8042.
36. Y. Filinchuk, Rönnebro, and D. Chandra, Acta Mater. **57**, (2009) 732.
37. Y. Lee, Y. Kim, Y. W. Cho, D. Shapiro, C. Wolverton, and V. Ozolins , Phys. Rev. B **79** (2009) 104107.
38. E. H. Majzoub and E. Rönnebro J. Phys. Chem. C, **113** (2009) 3352.
39. F. Buchter, Z. Łodziana, A. Remhof, O. Friedrichs, A. Borgschulte, Ph. Mauron, A. Züttel, D. Sheptyakov, L. Palatinus, K. Chopek, M. Fichtner, G. Barkhordarian, R. Bormann and B. Hauback, J. Phys. Chem. C **113** (2009) 17223.
40. S. Aldridge, A. J. Blake, A. J. Downs, R. O. Gould, S. Parsons, and C. R. Pulham, J. Chem. Soc., Dalton Trans. (1997) 1007.
41. M. Matsuo, Y. Nakamori, S.-I. Orimo, H. Maekawa, and H. Takamura, Appl. Phys. Lett. **91** (2007) 224103.
42. R. L. Corey, D. T. Shane, R. C. Bowman, Jr., ans M. S. Conradi J. Phys. Chem. C **112** (2008) 18706.
43. V. Ozolins, E. H. Majzoub, and C. Wolverton, Phys. Rev. Lett. **100** (2008) 135501.
44. J. Voss, J. S. Hummelshoj, Z. Łodziana and T. Vegge, J. Phys.: Condens. Matter, **21** (2009) 012203.

45. M. J. van Setten, G. A. de Wijs, M. Fichtner and G. Brocks, Chem. Mater. **20** (2008) 4952.
46. Y. Filinchuk, R. Cerný and H. Hagemann, Chem. Matter., **21** (2009) 925.
47. M. Fichtner, K. Chlopek, M. Longhini, and H. Hagemann, J. Phys. Chem. C **112** (2008) 11575.
48. A. Remhof, Z. Łodziana, F. Buchter, P. Martelli, F. Pendolino, O. Friedrichs, A. Züttel, J. P. Embs, J. Phys. Chem. C **113** (2009) 16384.
49. J. Mesot, S. Janssen, L. Holitzner and R. Hempelmann, J. Neutr. Res. **3** (1996) 293.
50. S. Janssen, J. Mesot, L. Holitzner, A. Furrer, and R. Hempelmann, Physica B **234–236** (1997) 1174.
51. J. D. Barnes, J. Phys. Chem **58** (1973) 5193.
52. R. E. Lechner, G. Badurek, A. J. Dianoux, H. Hervet, and F. Volino, J. Chem. Phys. **73** (1980) 934.
53. N. Jalarvo Department, A. Desmedt, R. E. Lechner, and F. Mezei, J. Chem. Phys. **125** (2006) 184513.
54. T. Tsang and T. C. Farrar, J. Chem. Phys., **50** (1969) 3498.
55. G. Kresse and J. Furthmüller, Comput. Mater. Sci. **6** (1996) 15.
56. P. E. Blöchl, Phys. Rev. B **50** (1994) 17953.
57. P. C. H. Mitchell, S. F. Parker, A. J. Ramirez-Cuesta, and J. Tomkinson, *Series on Neutron Techniques and Applications, Vol. 3, Vibrational Spectroscopy with Neutrons*, World Scientific Publishing, Singapore, 2005.
58. K. B. Harvey and N. R. McQuaker, Can. J. Chem. **49** (1971) 1971.
59. D. G. Allis and B. S. Hudson, Chem. Phys. Lett. **385** (2004) 166.
60. J. Tomkinson and T. C. Waddington, J. Chem. Soc. Faraday Trans. **2** (1976) 528.
61. S. Gomes , H. Hagemann, and K. Yvon, J. Alloys Compd. **346** (2002) 206.
62. A.-M. Racu, J. Schoenes, Z. Łodziana, A. Borgschulte, and A. Züttel, J. Phys. Chem. **112** (2008) 9716.
63. A. E. Shirk and D. F. Shriver, J. Am. Chem. Soc. **95** (1973) 5901.
64. M. I. Memon, W. F. Sherman, and G. R. Wilkinson, J. Raman Spec. **13** (1982) 96.
65. D. Chernyshov, A. Bosak, V. Dmitriev, Y. Filinchuk, and H. Hagemann, Phys. Rev. B **78** (2008) 172104.
66. P. Carbonnière and H. Hagemann, J. Phys. Chem. A **110** (2006) 9927.
67. H. Hagemann, Y. Filinchuk, D. Chernyshov, and W. van Beek, Phase Transitions, **82** (2009) 344.
68. K. L. Lindsay and B. Rouge, *Preparation of Alkali Metal Hydrides* US pat. 3,505,036 (1967).
69. B. Bogdanovic and M. Schwickardi, J. Alloys Comp. **253** (1997) 1.
70. D. L. Anton, J. Alloys Comp. **356** (2004) 400.
71. A. Leon, O. Kircher, J. Rothe, and M. Fichtner, J. Phys. Chem. B **108** (2004) 16372.
72. J. Graetz, J. J. Reilly, J. Johnson, A. Ignatov, A. Yu., and T. A. Tyson, Appl. Phys. Lett. **85** (2004) 500.
73. J. M. Bellosta von Colbe, W. Schmidt, M. Felderhoff, B. Bogdanovic, and F. Schueth, Angew. Chem. Int. Ed., **45** (2006) 3663.
74. Q. J. Fu, A. J. Ramirez-Cuesta, and S. C. Tsang, J. Phys. Chem. B, **110** (2006) 711.
75. W. Luo and K. J. Gross, J. Alloys Compounds. **385** (2004) 224.
76. K. J. Gross, G. J. Thomas, and C. M. Jensen, J. Alloys Compds. **330** (2002) 683.
77. O. Palumbo, R. Cantelli, A. Paolone, C. M. Jensen, and S. S. Srinivasan, J. Phys. Chem. B **109** (2005) 1168.
78. S. Singh, S. W. H. Eijt, J. Huot, W.A. Kockelmann, M. Wagemaker, and F. M. Mulder, Acta Mater. **55** (2007) 5549.
79. A. Borgschulte, A. Züttel, P. Hug, G. Barkhordarian, N. Eigen, M. Dornheim, R. Bormann, and A. J. Ramirez-Cuesta, Phys. Chem. Chem. Phys. **10** (2008) 4045.
80. Z. Łodziana, A. Züttel, J. Alloys Compds. **471** (2009) L29.

81. Z. Łodziana, A. Züttel, and P. Zielinski, J. Phys.: Condens. Matter **20** (2008) 465210
82. Y. Kawashima and E. Hirota, J. Chem. Phys. **96** (1992) 2460.
83. A. Borgschulte, A. Züttel, P. Hug, A.M. Racu, and J. Schoenes, J. Phys. Chem. A **112** (2008) 4749.
84. E. C. Ashby, F. R. Dobbs, and H. P. Hopkins, J. Am. Chem. Soc. **95** (1973) 2823.
85. S. Gomes, G. Renaudin, H. Hagemann, K. Yvon, M. P. Sulic, C. M. Jensen, J. All. Compds. **390** (2005) 305.
86. H. Yukawa, N. Morisaku, Y. Li, K. Komiy, R. Rong, Y. Shinzato, R. Sekine, and M. Morinaga, J. Alloys Compds. **446** (2007) 242.
87. H. Guynadin, K. N. Houk, and V. Ozolins, Proc. Natl. Acad. Sci. USA, **2008**, 10.1073/pnas.0709224105
88. R. Gremaud, Z. Łodziana, P. Hug, B. Willenberg, A.-M. Racu, J. Schoenes, A. J. Ramirez-Cuesta, K. Refson, A. Züttel, and A. Borgschulte, Phys. Rev. B **80** (2009) 100301.
89. D. T. Shane, R. C. Bowman and M. S. Conradi, J. Phys. Chem. C **113** (2009) 5039.
90. M. Cho, Chem. Rev. **108** (2008) 1331.